Protection heater design validation for the LARP magnets using thermal imaging

M. Marchevsky, M. Turqueti, D. W. Cheng, H. Felice, G. Sabbi, T. Salmi, A. Stenvall, G. Chlachidze, G. Ambrosio P. Ferracin, S. Izquierdo Bermudez, J. C. Perez, and E. Todesco

***Abstract*— Protection heaters are essential elements of a quench protection scheme for LARP high-field accelerator magnets. Various heater designs fabricated by LARP and CERN have already been tested in the LARP high-field quadrupole HQ, and presently being built into the coils of high-field quadrupole MQXF. In order to compare heat flow characteristics and thermal diffusion timescales of different heater designs, we powered heaters of two different geometries in ambient conditions and imaged resulting thermal distributions using a high-sensitivity thermal video camera. We observed peculiar spatial periodicity in the temperature distribution maps potentially linked to the structure of the underlying cable. 2D numerical simulation of heat diffusion and spatial heat distribution have been conducted, and results of the simulation and experiment have been compared. Imaging revealed hot spots formed due to a current concentration around high curvature points of heater strip of varying cross-section, and visualized thermal effects of various inter-layer structural defects. Thermal imaging can become a future quality control tool for the MQXF coil heaters.**

***Index Terms*—Quench Protection, Superconducting Magnets, Thermal Imaging**

I. Introduction

QUENCH PROTECTION of superconducting accelerator magnets is essential for their reliable operation. The goal of protection is to dissipate magnet stored energy quickly and uniformly upon detecting a quench, thus preventing possible performance degradation due to formation of a localized hot spot. This goal is accomplished through rapid heat injection into a magnet winding that brings it to a normal state. The most common method of heat injection is using "protection heaters" – thin polyimide sheets laminated with stainless steel that are impregnated with the winding and controlled by a current pulse [1]. Recently, another promising coil heating technique exploiting ac inter-filament coupling loss of superconducting cables has been developed [2]. A combination of these two techniques was shown to achieve best efficiency and shortest protection delay in a wide range of magnet operational currents [3]. Such combined protection approach is planned for the MQXF high-field Nb_3Sn magnets that are presently being built by US LARP and CERN collaboration for high-luminosity upgrade of the inner triplet of the LHC. [4]. MQXF-B being the largest 7.15 m long magnet of the triplet with a stored energy of 1.2 MJ/m at operational current, has a relatively narrow time margin [5] that dictates stringent protection requirement. Protection heaters efficiency thus needs to be optimized for reliable and redundant operation. There has been an effort to explore different heater geometries aiming at such optimization [6]. In this paper we focus on the two basic heater geometries that are relevant for MQXF, and have been implemented in the HQ03a LARP quadrupoles. We perform numerical simulations of heat diffusion and heat flux distribution in those geometries, conduct thermal video imaging, and compare the simulation and experiment results. Potential of thermal visualization as a quality control tool for the future MQXF heaters is also discussed.

II. MQXF heater options

A. Heater geometry options

The simplest protection heater geometry is a strip of uniform cross-section covering certain number of coil turns. Heaters of this type adapted to the coil layout were used in various HQ LARP quadrupole coils [7]. The advantage of a uniform strip heaters is that the entire length of the coil winding under it is being heated up simultaneously, and thus the only factor limiting such heater performance is the thermal diffusion time to propagate a sufficient temperature gradient into the cable through the insulation layer. This emphasizes importance of having a uniform and well-controlled properties of the interface, where variations of epoxy layer thickness and occasional inter-layer delamination may have profound effect on heater efficiency. While the uniform strip geometry is proven to work well in HQ magnet series, it cannot be directly adopted for a 7.15 meter long magnet, as net resistance of such long heater will rise prohibitively high for operating it at safe voltage levels. To overcome this problem, two approaches are been considered. In one, segments of the heater strip are over-

Automatically generated dates of receipt and acceptance will be placed here; authors do not produce these dates. Research supported by DOE via the US-LARP program and by the High Luminosity LHC project. A. Stenvall and T. Salmi were supported by Academy of Finland (grants: 250652 and 287027)

M Marchevsky (e-mail: mmartchevskii@lbl.gov), M. Turqueti, H. Felice, G. Sabbi are with the Lawrence Berkeley National Laboratory, Berkeley CA 94720 USA

T. Salmi was with Lawrence Berkeley National Laboratory Berkeley CA 94720 USA. She is now with the Department of Electrical Engineering, Tampere University of Technology, Tampere 33720 Finland.

A. Stenvall is with the the Department of Electrical Engineering, Tampere University of Technology, Tampere 33720 Finland

G. Chlachidze and G. Ambrosio are with the Fermi National Accelerator Laboratory, Batavia IL USA

P. Ferracin, S. Izquierdo Bermudez, J. C. Perez, and E. Todesco are with the European Center for Nuclear Physics (CERN), Geneva Switzerland.

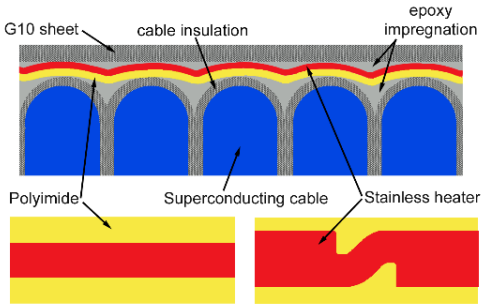

Fig. 1. Top: a cross-sectional view of the heater impregnated with the magnet coil. Bottom: two basic heater geometries used in LARP magnets, a strip of constant cross-section length (left), and a strip of a variable cross-section characterized by a periodic array of narrow width curved "heating stations" placed in-between the wide straight segments (right).

coated periodically with copper thus forming low resistance bridges between the stainless "heating stations". Alternative approach is to periodically vary a width of the heater strip along the coil, so that "heating stations" of higher resistance are formed such variation. This approach has been taken in LARP long quadrupole LQ [8], in one of the recent HQ02 coil [9], and is also considered as an option for the MQXF-L. A cross-sectional view of a protection heater trace impregnated with a superconducting coil, and the two basic design patterns discussed are shown in Fig 1.

B. 2D simulation of heat diffusion

Heat diffusion through insulation materials surrounding the heater can be readily calculated using finite element approach, by solving the heat equation iteratively using finite differences technique. This approach was used successfully to predict heat delays in various LARP magnets [10]. Here we use same technique to simulate heat diffusion at ambient conditions for a thin heater layer embedded in a composite insulation and placed on top of underlying superconducting cable. Our model geometry is a multi-layered stack (Fig. 2a) that includes a 25 mm thick stainless steel heater layer on a 50 mm thick polyimide substrate, separated at one side by a 100 mm layer of epoxy-impregnated cable insulation from two rounded copper blocks of 0.8 mm curvature radius. Stainless and polyimide layers are slightly undulated following the shape of the underlying cable turns. At the cable side, heater layer is facing a 150 mm thick layer of epoxy-impregnated cloth. For simplicity, heat diffusivities of epoxy, epoxy-impregnated cloth, and epoxy-impregnated cable insulation are considered the same. The temperature is fixed at the initial value of 295 K at all boundaries, while the outer face of the stack is separated from the nearest boundary by a 100 mm thick layer of very low (10^{-12} m^2/s) heat diffusivity emulating quasi-adiabatic condition at the surface open to the outside air. Radiative heat losses are ignored. Room temperature values of heat conductance and heat capacity for all materials were used. The simulation was performed with a constant time step of 0.1 μs, assuming uniform surface power density and exponential decay of heater current with a time constant of 20.25 ms (taken similar to the experimental value). Results are shown in Fig. 2 a-e. A peculiar evolution of the undulated temperature profile is observed:

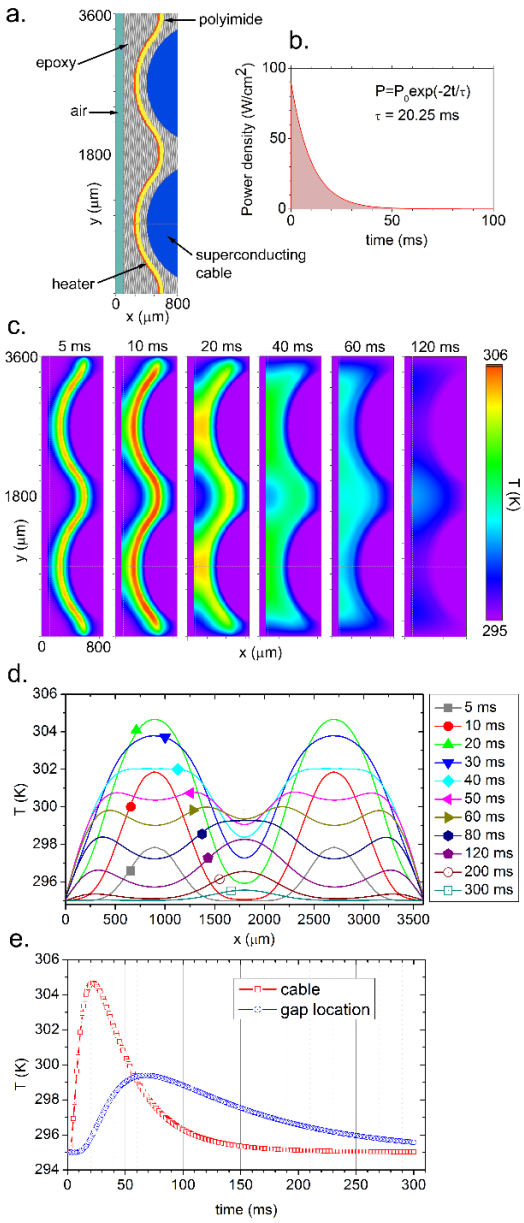

Fig. 2. (a) Heater stack setup used for the 2D heat diffusion simulation. (b) Time dependence of the heater power assumed for the simulation (c) A sequence of 2D heat maps calculated at various time intervals from the onset of heater firing. (d) Temperature profiles calculated along the outer surface of the heater stack at various time intervals. Surface temperature peaks initially seen at the locations where heater layer is pushed towards the stack surface, gradually transform into "dips" as heat is being removed into the underlying cable turns. (e) Time dependences of surface temperature at y=900 mm (cable location) and y=1800 μm (gap between the cable turns). Temperature peaks sequentially in those locations with a ~50 ms interval. Characteristic thermal relaxation times constants past the peak are ~35 ms and ~127 ms respectively.

the surface temperature initially peaks at the locations closest to heater surface, but later on the profile becomes inverted as peaks transform to valleys and new temperature maxima arise at locations in-between the cable turns.

Effect of curvatures to the heating power distribution

An important additional source of inhomogeneous lateral heat deposition in the heater of variable cross-section is a

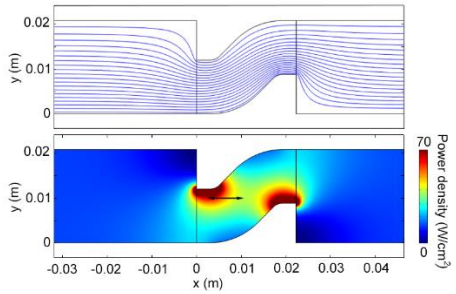

Fig. 3. (a) Result of a simulation for the current flow lines (top) and surface power distribution (bottom) in a single period of a heater strip of variable cross-section. Power deposition peaks locally at the curvature end points. A relative temperature rise from the middle of the heating station towards the hot spot along the central line (depicted with an arrow) is ~ 58%

non-uniform current distribution near the curvature points at the heating station ends. This distribution can be readily derived using equipotential lines approach. In Fig. 3 results of current flow and heating power calculation performed in Comsol for a single heating station biased with 10 V is shown. Current flow concentrates near the curvature end points resulting in a formation of localized hot spots. As our heat diffusion simulation assumed a uniform power density across the heater, it is an important next step to understand how the curvature point hot spots may affects thermal diffusion time and ultimately, the protection performance.

III. THERMAL IMAGING

Thermal imaging is an efficient tool for mapping temperature distribution and identifying thermal inhomogeneity. We used this technique to measure time-dependent temperature distribution in different heater patterns and compare the measurements to our simulation results. Time-resolved video sampling of thermal images allows to directly evaluate thermal diffusion rate, and detect spatial variation of heat diffusivity. For our experiments we used a Keysight U5855A TrueIR Thermal Imager camera with 0.1 K sensitivity interfaced to a PC-based frame grabber software. The camera was installed on a tripod above the magnet coil, facing the heater strip. Heater was powered with a unit containing a capacitor that was initially charged to 150-350 V and then discharged into the heater strip using a manually-triggered SCR circuit, resulting in characteristic power densities of ~50-200 W/cm^2 in the heater. IR images were acquired continuously throughout the heater firing and the following thermal relaxation process by the camera at 9 frames/s internal rate and the video stream was up-sampled to 25 frames/s by a PC software.

A. Imaging of the QXF-style heater of variable cross-section

We performed time-resolved thermal imaging on the outer layer heater of variable cross-section with periodic heating stations. An identical heater was installed on the HQ Coil 26 of HQ03a LARP quadrupole; a spare coil was used for imaging studies. Heaters were formed with photolithography in 25 μm thick stainless steel, and laminated over 50 μm thick polyimide film. The heater was impregnated to the coil wound with 1.6 mm thick Nb_3Sn Rutherford cable insulated with 100 μm thick layer of S-glass. The insulation on top of the heater is ~150 μm thick. Each heating station is 12 mm wide and spans at 45 deg. angle in-between the 20.8 mm wide straight strip sections. A photograph of the heating station is shown in Fig 4a. An undulated surface profile of the stainless layer following the underlying cable structure is clearly visible through the optically-transparent top layer of epoxy-impregnated insulation. One should note, however, that insulation transparency in the wavelength interval of 8-14 μm relevant for thermal imaging is quite small, and therefore only the exposed top surface of the insulation layer is being imaged in our experiments. The heater was pulsed using a capacitor bank of 0.56 mF charged to 300 V, yielding a 85 A spike of heater current followed by decay with time constant of 20.25 ms. Imaging result is shown in Fig. 4b. One can clearly distinguish the periodic thermal modulation caused by the varying distance between the heater and the top insulation layer. The measured temperature distribution period of 1.75 mm, as seen from the A-B cross-sectional plot (Fig. 4c), matches the expected inter-turn separation of ~1.8 mm. Two hot spots are observed around the curved end points of the heating station. Temperature rise from the center of the heating station towards the hot spot measured along the median C-D line is ~6.0 K (Fig. 4d), or when normalized to T_D-T_A, it is 50% - in good agreement with the simulation result. An impregnation defect causing the heater layer to wrinkle and slide deeper into the groove between neighboring turns is also clearly revealed in the thermal image (shown with arrows in Fig. 4a and Fig. 4b.). Its dark appearance is consistent with a thicker layer of impregnation epoxy separating heater from the top surface. Images of temporal evolution of the surface temperature are shown in Fig. 5.

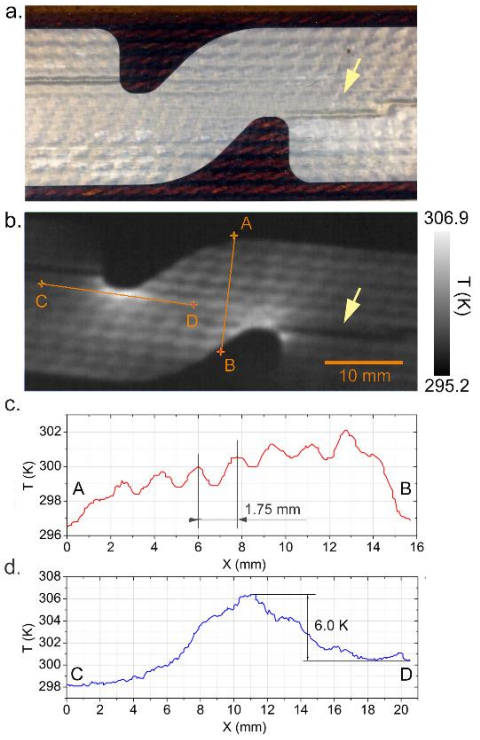

Fig. 4. (a) Photograph of the heating station at the coil outer surface. (b) The first thermal image taken past the current spike in the heater. (c) Temperature distribution in the direction perpendicular to the turns. A periodic distribution pattern resembling the underlying cable structure is seen. (d) Temperature distribution along the median line showing temperature rise towards a hotspot.

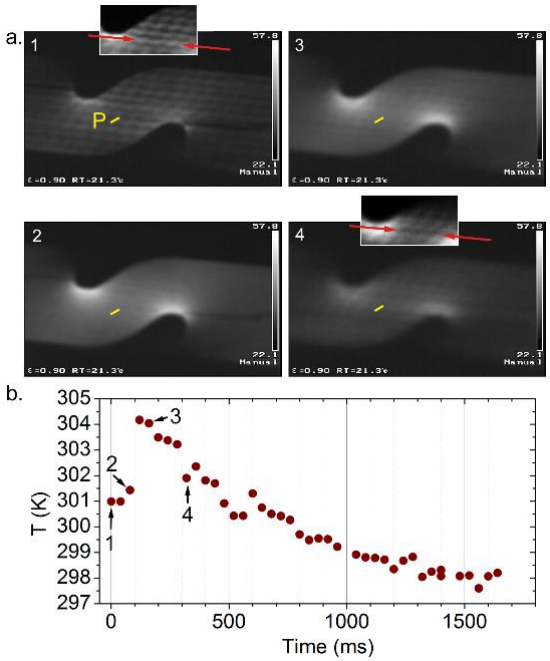

Fig. 5. (a) Thermal images (direct camera views) taken sequentially past the heater powering with time intervals of t_{12} and t_{23} of 80 ms and t_{34} of 160 ms. A zoomed-in region near the hot-spot showing details of the modulated pattern is shown in the insets of Images 1 and 4. (b) Temporal evolution of the temperature calculated by averaging values along a 10 pixel line (marked "P) in the middle of the heating station. Data points corresponding to the images shown in (a) are labeled.

As heater power is decreasing to zero, a more uniform distribution without a pronounced short-scale modulation emerges (Image 2). Later on, as heat is being removed into the cable, a modulated pattern re-emerges again (Image 4), but now it is inverted with respect to the initial one, as shown in the insets of Images 1 and 4. This is in agreement with our heat diffusion simulation results. A thermal relaxation time constant extracted from the data in Fig. 5b is ~685 ms. This is substantially longer than that obtained in the simulation, thus suggesting a poorer thermal interface contact between the heater and its neighboring layers, or a thicker than expected layer of insulation (including the epoxy) built into the heater stack during impregnation.

B. Imaging of the HQ-style heater of constant cross-section.

An HQ-style strip heater of constant width installed at the inner layer of HQ02 coil has been imaged after that coil removal from HQ02 magnet following two magnet cold tests. As heater strips were fired over hundred times during magnet training and quench heater studies, they developed numerous local delamination defects. An example is shown in the photograph of Fig. 6a. Upon firing this heater (at capacitor voltage 350 V, time constant ~40 ms), thermal imaging revealed such defects clearly (Fig. 6b). For example, the central portion of the U-shaped heater part exhibits a heavily delaminated area; in thermal images it initially stays dark for up to ~600 ms thus suggesting a delamination between the heater and top layer of insulation. But after ~3000 ms pass, most of the heater strip cools down while the area of interest stays warm and eventually

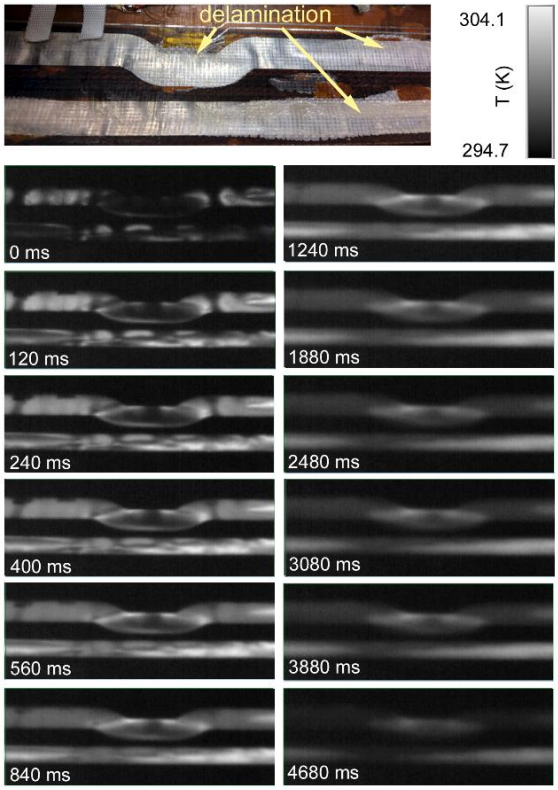

Fig. 6. (a) A photograph of the HQ Coil 20 inner layer heater exhibiting delamination defects (marked with arrows) after two magnet cold tests. (b) A sequence of thermal images showing strong inhomogeneity of thermal distribution due to delamination defects, and its temporal evolution. Labels show elapsed time intervals relative to the first acquired image.

turns bright in the image. It is therefore plausible to assume that thermal contact between the heater layer and the coil is also poor in that area, hinting at delamination been present at both sides of the heater. While it is hard to distinguish by visual inspection which side of the heater is delaminated, thermal imaging provides an alternative non-destructive way of doing this determination.

IV. Conclusion

Thermal imaging is a direct and sensitive technique to characterize heat diffusion in the impregnated heaters of high-field accelerator magnets. Fine-scale spatial modulation of a thermal distribution can be used as a sensitive probe for accessing uniformity of the heater stack. Timed acquisition of thermal images allows probing the local thermal diffusion characteristics of the heater stacks and facilitates non-destructive qualification of delamination defects. Thermal imaging appears to be a promising and useful technique for quality assurance evaluation of future QXF coils during production, as well as for nondestructive evaluation of heater defects caused by their operation in magnet cold tests.

Acknowledgment

Authors are thankful to J. Swanson and T. Lipton for assistance in coil preparation.

REFERENCES

[1] H. Felice, G. Ambrosio, G. Chlachidze, P. Ferracin, R. Hafalia, R. C. Hannaford, J. M. Joseph, A. F. Lietzke, A. D. McInturff, J. F. Muratore, S. Prestemon, G. L. Sabbi, J. Schmalzle, P. Wanderer, and X. R. Wang, "Instrumentation and quench protection for LARP Nb3Sn magnets," IEEE Trans. Appl. Supercond., vol. 19, no. 3, pp. 2458–2462, Jun. 2009.

[2] E. Ravaioli, V. I. Datskov, C. Giloux, G. Kirby, H. H. J. ten Kate, and A. P. Verweij, "New, coupling loss induced, quench protection system for superconducting accelerator magnets," IEEE Trans. Appl. Supercond., vol. 24, no. 3, Jun. 2014, Art. ID. 0500905.

[3] E. Ravaioli, H. Bajas, V. I. Datskov, V. Desbiolles, J. Feuvrier, G. Kirby, M. Maciejewski, G. Sabbi, H. H. J. ten Kate, and A. P. Verweij, "Protecting a Full-Scale Nb3Sn Magnet With CLIQ, the New Coupling-Loss-Induced Quench System for high-luminosity upgrade of the inner triplet of the LHC.", IEEE Trans. Appl. Supercond., vol. 25, no. 3, Jun 2015, Art. ID 4001305.

[4] G.Ambrosio, "Nb3Sn High Field Magnets for the High Luminosity LHC Upgrade Project", IEEE Trans. Appl. Supercond., vol. 25, no. 3, Jun 2015, Art. ID 4002107.

[5] E. Todesco, "Quench limits in the next generation of magnets", Proceedings of the WAMSDO Workshop, CERN 2013.

[6] T. Salmi, G. Ambrosio, S. Caspi, G. Chlachidze, H. Felice, M. Marchevsky, S. Prestemon, and H. H. J. ten Kate, "Protection Heater Delay Time Optimization for High-Field Nb3Sn Accelerator Magnets", IEE Trans. Appl. Supercond., vol. 24, no. 3, Jun. 2014, Art. ID 4701305

[7] H. Felice, G. Ambrosio, M. Anerella, R. Bossert, S. Caspi, D. W. Cheng, D. R. Dietderich, P. Ferracin, A. K. Ghosh, R. Hafalia, C. R. Hannaford, V. Kashikhin, J. Schmalze, S. Prestemon, G. Sabbi, P.Wanderer, and A.V. Zlobin "Design of HQ—A High Field Large Bore Nb3Sn Quadrupole Magnet for LARP", IEEE Trans. Appl. Supercond., vol. 19, no. 3, pp. 1235-1239, Jun. 2009.

[8] G. Ambrosio, N. Andreev, M. Anerella, E. Barzi, R. Bossert, S. Caspi, G. Chlachidize, D. Dietderich, S. Feher, H. Felice, P. Ferracin, A. Ghosh, R. Hafalia, R. Hannaford, V. V. Kashikhin, J. Kerby, M. Lamm, A. Lietzke, A. McInturff, J. Muratore, F. Nobrega, I. Novitsky, G. L. Sabbi, J. Schmalzle, M. Tartaglia, D. Turrioni, P. Wanderer, G. Whitson, and A. V. Zlobin, "LARP Long Nb3Sn Quadrupole Design", IEEE Trans. Appl. Supercond., vol. 18, no. 2, pp. 268-272, Jun. 2008

[9] J. DiMarco, G. Ambrosio, M. Anerella, H. Bajas, G. Chlachidze, F. Borgnolutti, R. Bossert, D.W. Cheng, D. Dietderich, H. Felice, P. Ferracin, A. Ghosh, A. Godeke, A. R. Hafalia, M. Marchevsky, D. Orris, E. Ravaioli, G.L. Sabbi, T. Salmi, J. Schmalzle, S. Stoynev, T. Strauss, C. Sylvester, M. Tartaglia, E. Todesco, P. Wanderer, X.R. Wang, M. Yu, "Test Results of the LARP HQ03a Nb3Sn Quadrupole", this issue of IEEE

[10] T. Salmi, D. Arbelaez, S. Caspi, H. Felice, M. G. T. Mentink, S. Prestemon, A. Stenvall, and H. H. J. ten Kate, "A Novel Computer Code for Modeling Quench Protection Heaters in High-Field Nb3Sn Accelerator Magnets", IEEE Trans. Appl. Supercond, vol. 24, no. 5, Aug. 2014, Art. ID 4701810.